RSC Advances

PAPER

View Article Online
View Journal | View Issue

Cite this: *RSC Adv.*, 2020, **10**, 30848

Synthesis of 1,3,4-oxadiazoles derivatives with antidepressant activity and their binding to the 5-HT_{1A} receptor†

Shiben Wang,[a] Lin Qi,[b] Hui Liu,[c] Kang Lei,[a] Xuekun Wang[a] and Renmin Liu*[a]

Received 6th July 2020
Accepted 6th August 2020

DOI: 10.1039/d0ra05886f

rsc.li/rsc-advances

In this study, two series of 1,3,4-oxadiazole derivatives were designed and synthesized using the forced swimming test (FST) model to test the antidepressant activity of the target compound *in vivo*. Five compounds with potential activity were selected from the FST model to test affinity with 5-HT_{1A} receptor *in vitro*. The results of the FST experiment showed that compound *N*-(3-((5-((4-chlorobenzyl) thio)-1,3,4-oxadiazol-2-yl)methoxy)phenyl)acetamide (**10g**) showed the best antidepressant activity (DID = 58.93, percentage decrease in immobility duration in FST), similar to the activity of positive drug fluoxetine. Compound **10g** also exhibited the most potent binding affinity to 5-HT_{1A} receptors (K_i = 1.52 nM). The results of the *in vivo* 5-HT concentration estimation in mice showed that compound **10g** may have an effect on the brain. The experimental results of exploratory activity in mice showed that compound **10g** did not affect spontaneous activity in the open-field test model. Molecular docking was used to study the binding mode of compound **10g** and the 5-HT_{1A} receptor. Compound **10g** showed significant interactions with residues at the active site on the 5-HT_{1A} receptor. The physicochemical and pharmacokinetic properties of the target compounds were predicted using Discovery Studio 2019 and ChemBioDraw Ultra 14.

1. Introduction

Depression has become a major public health problem at present, with high prevalence, high suicide rate and significant societal costs.[1,2] Currently, drug therapy is the main method of depression treatment. Some patients can be treated with drugs, but some patients still need to take drugs for a long time, but long-term use will have side effects, including affecting sleep quality, weight gain, gastrointestinal bleeding, *etc.* It also results in substantial healthcare costs.[3,4] Therefore, there is an urgent need to search for new strategies for treatment of this disease.

Derivatives containing 1,3,4-oxadiazole structure are widely used in antidepressant drug research. For example, Singh *et al.*, designed and synthesized a series of 1,3,4-oxadiazole derivatives, which showed good antidepressant activity.[5] In addition, 3,4-dihydroquinolin-2(1*H*)-one also is a promising fragment in antidepressant drug research. For example, Deng *et al.*, designed and synthesized a series of 3,4-dihydroquinolin-2(1*H*)-one derivatives, which showed good antidepressant activity (Fig. 1).[6] In our previous studies, we designed and synthesized a series of 3,4-dihydroquinolin-2(1*H*)-one derivatives.[7] Pharmacological experiment results show that this series of compounds showed good antidepressant activity in forced swimming test (FST) model. The preliminary mechanism of action indicates that it acts on the 5-hydroxy tryptamine 1A (5-HT_{1A}) receptor and produces antidepressant activity. In this study, we adopted this series of compounds as lead compounds, combined structural fragments of 1,3,4-oxadiazole and 3,4-dihydroquinolin-2(1*H*)-one to improve their efficacy on depression, and a series of compounds **5a–i** were designed and synthesized. To investigate the importance of the 3,4-dihydroquinolin-2(1*H*)-one fragment in the compound, a series of

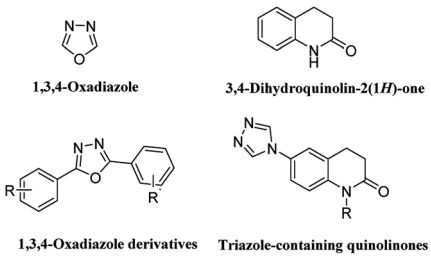

Fig. 1 The chemical structure of 1,3,4-oxadiazole, 3,4-dihydroquinolin-2(1*H*)-one, and their derivatives.

[a]College of pharmacy, Liaocheng University, Liaocheng, Shandong 252059, China. E-mail: wangshiben110@163.com

[b]Railway Police College, Zhengzhou, Henan 450053, China

[c]College of Life Sciences, Liaocheng University, Liaocheng, Shandong 252059, China

† Electronic supplementary information (ESI) available. See DOI: 10.1039/d0ra05886f

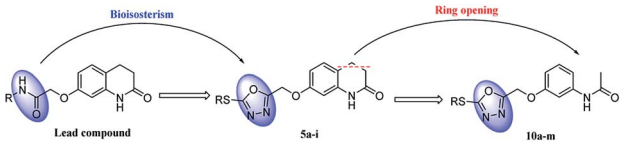

Fig. 2 Structures of target compound **5a–i** and **10a–m**.

derivatives **10a–m** were designed and synthesized by cutting at the 3 and 4 positions of 3,4-dihydroquinolin-2(1*H*)-one and by increasing the flexibility of the molecule to investigate the effect of ring opening on the compound activity (Fig. 2).

In this study, we used FST model, to test the antidepressant activity of the target compound *in vivo*. And 5-HT_{1A} receptor binding assay was performed to determine the possible mechanism of action of the potent compound. The most potential compounds that showed effectiveness in FST, and the 5-HT concentration evaluation experiment was performed to test for their effect on 5-hydroxytryptamine (5-HT, serotonin) concentration in the mice brain, by using ELISA. The exploratory activity of the animals was also evaluated by the open-field test. The molecular docking module in the computer software Discovery Studio (DS) 2019 was used to analyze the possible modes of action of the potential compounds and 5-HT_{1A} receptor active sites. Simultaneously, DS 2019 and ChemBio-Draw Ultra 14.0 were used to predict the physicochemical and pharmacokinetic properties of the target compound. To confirm the structure of the target compound, we used high resolution mass spectrometry (HRMS) and ^{1}H-nuclear/^{13}C-nuclear magnetic resonance technology.

2. Results and discussion

2.1 Chemistry

The synthetic routes of target compounds **5a–i** and **10a–m** are shown in Schemes 1 and 2. First, intermediates **2** and **7** were synthesized under similar reaction conditions. Under reflux conditions, 7-hydroxy-3,4-dihydroquinolin-2(1*H*)-one/*N*-(3-hydroxyphenyl)acetamide was reacted with $BrCH_2CO_2CH_3$ to obtain intermediates **2** and **7**. Secondly, intermediates **2** and **7** were reacted with hydrazine hydrate using THF as a solvent, and intermediates **3** and **8** were obtained by reaction under reflux

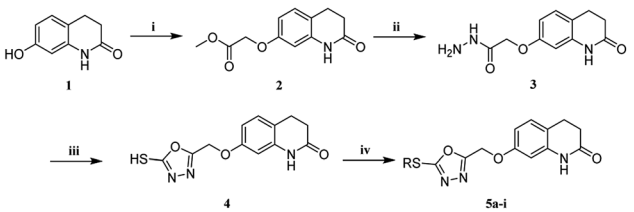

Scheme 1 Synthesis of the target compounds **5a–i**. Substituent R: **5a**: *n*-C_4H_9; **5b**: *n*-C_5H_{11}; **5c**: *n*-C_6H_{13}; **5d**: *n*-C_7H_{15}; **5e**: CH_2Ph; **5f**: CH_2Ph (*p*-F); **5g**: CH_2Ph (*p*-Cl); **5h**: CH_2Ph (*p*-CF_3); **5i**: CH_2Ph (*p*-CH_3). Reagents and conditions: (i) $BrCH_2CO_2CH_3$, K_2CO_3, CH_3CN; reflux, 6–8 h; (ii) $NH_2NH_2.H_2O$, THF, reflux, 2 h; (iii) NaOH, CS_2, C_2H_5OH, 80 °C, 19–21 h; (iv) RBr, K_2CO_3, acetone, 65 °C, 10 h.

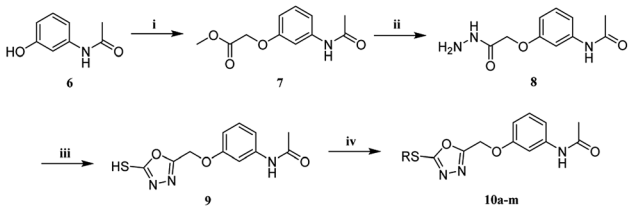

Scheme 2 Synthesis of the target compounds **10a–m**. Substituent R: **10a**: CH_2Ph; **10b**: CH_2Ph (*o*-F); **10c**: CH_2Ph (*m*-F); **10d**: CH_2Ph (*p*-F); **10e**: CH_2Ph (*o*-Cl); **10f**: CH_2Ph (*m*-Cl); **10g**: CH_2Ph (*p*-Cl); **10h**: CH_2Ph (*o*-CF_3); **10i**: CH_2Ph (*m*-CF_3); **10j**: CH_2Ph (*p*-CF_3); **10k**: CH_2Ph (*o*-CH_3); **10l**: CH_2Ph (*m*-CH_3); **10m**: CH_2Ph (*p*-CH_3). Reagents and conditions: (i) $BrCH_2CO_2CH_3$, K_2CO_3, CH_3CN; reflux, 6–8 h; (ii) $NH_2NH_2.H_2O$, THF, reflux, 2 h; (iii) NaOH, CS_2, C_2H_5OH, 80 °C, 19–21 h; (iv) RBr, K_2CO_3, acetone, 65 °C, 10 h.

conditions. Next, intermediates **4** and **9** were generated *via* cyclization of intermediates **3** and **8** with CS_2 under basic conditions. Following this process resulted in an incomplete reaction, and extra CS_2 had to be added after 5–10 h to complete the reaction. The synthesis methods of intermediates **4** and **9** were synthesized according to the reported literature.[8] Intermediates **4** and **9** were reacted with bromides to obtain target compounds **5a–i** and **10a–m**. The structures of all target compounds **5a–i** and **10a–m** were confirmed by ^{1}H, ^{13}C, and HRMS technology.

2.2 Pharmacology

2.2.1. FST. The target compounds **5a–i** and **10a–m** were screened for antidepressant activity using FST model (dose: 40 mg kg; test time: 0.5 h). Fluoxetine was used as positive control drug in FST model. The results of the pharmacological experiments showed that most of the target compounds showed good antidepressant activity in the FST experimental model. The antidepressant activity of all target compounds are shown in Table 1.

The pharmacological data of target compounds **5a–i** and **10a–m** in FST model are shown in Table 1. As shown in Table 1. Most of compounds showed antidepressant activity at doses of 40 mg kg^{-1}, with nine compounds, namely **5f**, **10a–d**, **10f**, **10h–i**, and **10m** showing significant ($p < 0.05$, compared with the control group) antidepressant activity. Five compounds, namely **5g–h**, **10e**, **10g**, and **10j** showing high significant ($p < 0.01$, compared with the control group) antidepressant activity. Moreover, other compounds showed weak antidepressant activity. Especially, alkyl chain substituted compounds in the series of compounds **5a–i**.

The pharmacological results in Table 1 show that in the FST model, compound **10g** showed the best antidepressant activity, reduced the immobility time of the mice to 64.35 s, and its antidepressant activity was similar than that of fluoxetine (67.31 s). To explore the relationship between activity and compound dose, compounds **10g** and fluoxetine were screened for antidepressant activity using three dose groups: 10, 20, and 40 mg kg^{-1}, respectively. The pharmacological results show that

Table 1 Antidepressant activities of compounds **5a–i** and **10a–m** in FST

Compounds	R	Antidepressant activities[a] Duration of immobility (s) (mean ± SEM)[b]	DID[c] (%)
5a	C_4H_9	132.23 ± 13.12	15.62
5b	C_5H_{11}	105.76 ± 18.45	32.51
5c	C_6H_{13}	141.56 ± 20.38	9.67
5d	C_7H_{15}	126.45 ± 21.77	19.31
5e	CH_2Ph	128.83 ± 10.87	17.79
5f	CH_2Ph (*p*-F)	99.87 ± 20.41[d]	36.27
5g	CH_2Ph (*p*-Cl)	67.24 ± 18.37[e]	57.09
5h	CH_2Ph (*p*-CF_3)	75.04 ± 15.31[e]	52.11
5i	CH_2Ph(*p*-CH_3)	101.84 ± 20.41	35.01
10a	CH_2Ph	94.61 ± 18.87[d]	39.63
10b	CH_2Ph (*o*-F)	85.27 ± 21.19[d]	45.59
10c	CH_2Ph (*m*-F)	90.51 ± 15.69[d]	42.24
10d	CH_2Ph (*p*-F)	82.27 ± 17.29[d]	47.50
10e	CH_2Ph (*o*-Cl)	72.80 ± 16.12[e]	53.54
10f	CH_2Ph (*m*-Cl)	84.81 ± 20.39[d]	45.88
10g	CH_2Ph (*p*-Cl)	64.35 ± 17.48[e]	58.93
10h	CH_2Ph (*o*-CF_3)	87.10 ± 14.67[d]	44.42
10i	CH_2Ph (*m*-CF_3)	83.34 ± 18.70[d]	46.82
10j	CH_2Ph (*p*-CF_3)	74.71 ± 18.88[e]	52.32
10k	CH_2Ph (*o*-CH_3)	132.21 ± 22.20	15.63
10l	CH_2Ph (*m*-CH_3)	106.45 ± 19.96	32.07
10m	CH_2Ph (*p*-CH_3)	95.27 ± 16.61[d]	39.21
Fluoxetine	—	67.31 ± 11.47[e]	57.05
Control	—	156.72 ± 19.09	—

[a] Target compounds and Fluoxetine were administered at 40 mg kg^{-1}. [b] Values represent the mean ± SEM ($n = 8$). [c] %DID: percentage decrease in immobility duration. [d] Significantly compared to control ($0.01 < p < 0.05$). [e] Very significantly compared to control ($p < 0.01$).

within a certain dose range, as the dose increases, the antidepressant activity increases (Fig. 3).

2.2.2. TST. The tail suspension test (TST) model is another effective way to screen antidepressants. In order to verify the effectiveness of compound **10g**, we used the TST experimental model to further test the antidepressant activity of the compound. The pharmacological data of compound **10g** in TST model is shown in Fig. 4. As shown in Fig. 4, compound **10g** showing highly significant ($p < 0.01$, compared with the control group) antidepressant activity at 40 mg kg^{-1}.

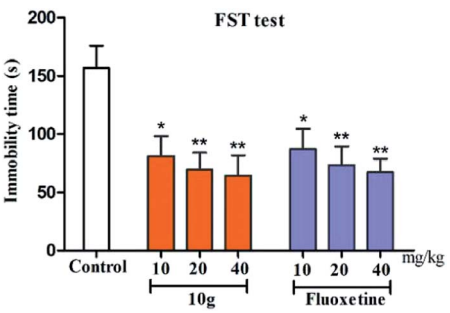

Fig. 3 Antidepressant activities of compound **10g** and fluoxetine in FST at different doses (40, 20, 10 mg kg^{-1}). Values represent the mean ± SEM ($n = 8$). * Significantly compared to control ($0.01 < p < 0.05$). ** Very significantly compared to control ($p < 0.01$).

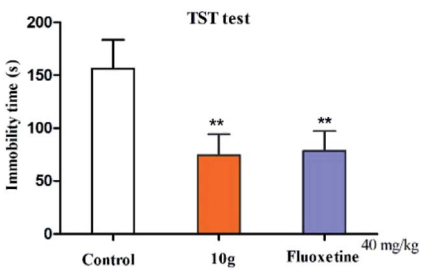

Fig. 4 Antidepressant activities of compound **10g** and fluoxetine in the TST test (40 mg kg^{-1}). Values represent the mean ± SEM ($n = 8$). * Significantly compared to control ($0.01 < p < 0.05$). ** Very significantly compared to control ($p < 0.01$).

2.2.3. Determination of 5-HT concentration. The content and dysfunction of monoamine neurotransmitter 5-HT in the central nervous system may be related to the onset of various diseases such as psychosis, migraine, depression and so on. Studies have shown that 5-HT may be related to the neurobiochemical mechanism of depression. Pathological autopsy results of depression show that 5-HT levels in the brain stem and frontal lobe are reduced, and the total amount of 5-HT receptors in the hippocampus is reduced.[9] In this study, 5-HT concentration is determined by enzyme-linked immunosorbent assay (ELISA) method. As shown in Fig. 5, at dose of 40 mg kg^{-1}, compound **10g** and fluoxetine significantly ($p < 0.05$) increased

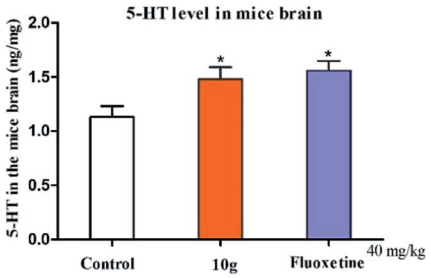

Fig. 5 Effect of compound **10g** and fluoxetine on brain 5-HT level in mice (40 mg kg^{-1}). Compound **10g** and fluoxetine were analyzed (the concentration of 5-HT in the mice brain) 1 h after oral administration. Represent the mean ± SEM ($n = 8$). * Significantly compared to control ($0.01 < p < 0.05$).

the 5-HT concentration in the mice compared with the control group. The results showed that compound **10g** may have a certain effect on the 5-HT system, as it increased the 5-HT concentration in the brain of mice.

2.2.4. Open-field test. The open field test is a method for evaluating the behavior of experimental animals in a new environment, exploring behavior and tension. The frequency and duration of certain behaviors of the experimental animals in the novel environment reflect the autonomous behavior and inquiry behavior of the experimental animals in the strange environment.

In the animal models of behavioral despair and depression, the shortening of animal immobility time is related to drug excitement sympathetic nerves.[10,11] In this experiment, open field test was used to verify whether compound **10g** can increase central excitability and affect the spontaneous activity of animals (this experiment examines spontaneous activities including: crossing, rearing, and grooming). The results of pharmacological showed that compound **10g** had no significant difference ($p > 0.5$) compared to the control in the crossing, rearing, and grooming tests, and did not affect the spontaneous locomotor activity of mice (Fig. 6). The results of this experiment excluded that compound **10g** is a false positive in mice due to excitatory central activity.

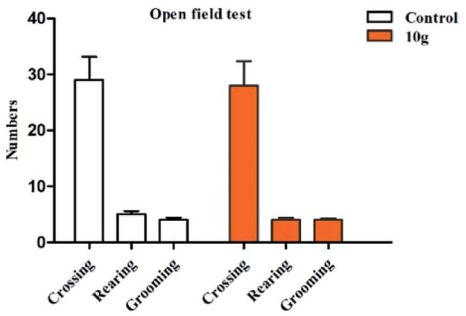

Fig. 6 Exploratory activity (counts) in the open-field test. Compound **10g** (40 mg kg^{-1}) was administered 1 h before the test. Locomotion: number of line crossings; rearing: number of times seen standing on hind legs; grooming: number of modifications. The values represent the mean ± SEM ($n = 8$).

Table 2 5-HT_{1A} receptor binding of selected compounds and reference serotonin

Compounds	5-HT_{1A} (K_i [nM] ± SEM)[a]
5g	1.77 ± 0.14
5h	2.73 ± 0.22
10e	2.01 ± 0.18
10g	1.68 ± 0.13
10j	4.14 ± 0.16
Serotonin	1.65 ± 0.11

[a] K_i values were obtained from 8 concentrations of the compound, each in duplicate.

2.2.5. 5-HT_{1A} receptor binding assay. The 5-HT_{1A} receptor plays an important role in the pathogenesis of various mental and neurological diseases. Activation of postsynaptic 5-HT_{1A} receptors is important for the favorable response to antidepressants.[12,13] In this study, five potential compounds, **5g**, **5h**, **10e**, **10g**, and **10j** were selected from FST model, and their affinities for the 5-HT_{1A} receptor were determined to further study their possible mode of action. The K_i value of the compounds were determined using this experiment. The pharmacological results are shown in Table 2. As shown in Table 2, all compounds showed strong affinities for the 5-HT_{1A} receptor, and compound **10g** showed highest affinities for the 5-HT_{1A} receptor, and its K_i value was 1.68 nM, similar to native neurotransmitter serotonin ($K_i = 1.65$ nM).

2.2.6. Structure–activity relationships. In this study, we used the previously synthesized 3,4-dihydroquinolin-2(1*H*)-one derivatives as lead compound, and combined structural fragment of 1,3,4-oxadiazole to improve their efficacy on depression, and a series of compounds **5a–i** were designed and synthesized. To investigate the importance of the 3,4-dihydroquinolin-2(1*H*)-one fragment in the compound, a series of derivatives **10a–m** were designed and synthesized by cutting at the 3 and 4 positions of 3,4-dihydroquinolin-2(1*H*)-one and by increasing the flexibility of the molecule to investigate the effect of ring opening on the compound activity. Screen the pharmacological activity of the target compound by FST model. The obtained compounds with better activity were further studied. Based on the pharmacological results obtained, the structure–activity relationships (SARs) of the target compounds were analyzed (Fig. 7).

Fig. 7 SARs of target compounds **5a–i** and **10a–m**. SARs for antidepressant activity of target compounds **5a–i** and **10a–m** at the R substituent: (1) benzyl-substituted derivatives are better than alkyl-substituted derivatives; (2) benzyl-substituted derivatives: *p*-F > *o*-F > *m*-F, *p*-Cl > *o*-Cl > *m*-Cl, *p*-CF_3 > *o*-CF_3 > *m*-CF_3, *p*-CH_3 > *m*-CH_3 > *o*-CH_3; (3) compounds substituted by Cl and CF_3 groups on the benzene ring was superior to the compound substituted by F and CH_3.

The pharmacological results obtained for compounds **5a–i** showed that among the alkyl chain C_4–C_7-substituted compounds, all compounds showed weak antidepressant activity, compared with the control group, and it is not significant. For benzyl-substituted derivatives, the *p*-Cl substituted compound showed the best antidepressant activity than F-, CF_3-, and CH_3-substituted compounds. Overall, the antidepressant activity of the benzyl-substituted derivatives was superior to that of the alkyl chain-substituted derivatives. In view of the poor activity of alkyl chain substituted compounds in **5a–i**, we only designed and synthesized benzyl substituted compounds in **10a–m**. The pharmacological results of compounds **10a–m** showed that among the benzyl-substituted derivatives, the activity of derivatives with different electronic group on the benzene ring was in the following order: *p*-F > *o*-F > *m*-F, *p*-Cl > *o*-Cl > *m*-Cl, *p*-CF_3 > *o*-CF_3 > *m*-CF_3, *p*-CH_3 > *m*-CH_3 > *o*-CH_3. The antidepressant activity of benzyl-substituted derivatives was superior to that of the alkyl chain-substituted derivatives.

By observing the pharmacological activities of **5a–i** and **10a–m**, it was found that the activity of compounds substituted by Cl and CF_3 groups on the benzene ring was superior to the compounds substituted by F and CH_3. It may be that the introduction of Cl and CF_3 groups on the benzene ring has a greater influence on the charge distribution of the compound, which is conducive to the electrical binding of the compound and the receptor. Secondly, the introduction of Cl and CF_3 groups on the benzene ring can increase the compound's liposolubility, and then make it easier to enter the brain tissue and play an antidepressant effect.

2.2.7. Docking study. In recent years, molecular docking, a theoretical simulation method that mainly studies intermolecular interactions and predicts the binding mode and affinity, has become an important technology in the field of computer-aided drug study. The most active compound **10g**, native neurotransmitter serotonin, and the active site of the 5-HT_{1A} receptor homology model were selected for molecular docking studies. The molecular docking module (Libdock) in the DS 2019 software was used for docking analysis. The results of molecular docking are shown in Fig. 8.

According to the literature, the main amino acids around the active site are Ala93, Gln97, Phe112, Ile113, Asp116, Val117, Cys120, Thr121, Ile124, Ile189, Thr196, Ser199, Thr200, Ala203, Phe361, Phe362, Ala365, Thr379, Gly382, Ala383, and Asn386.[14]

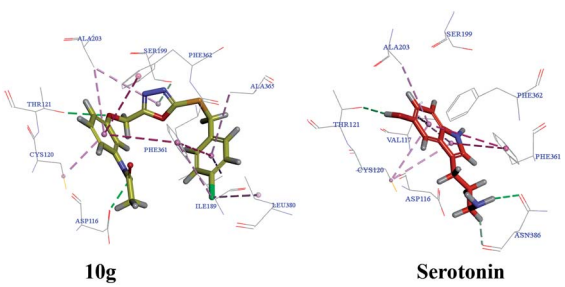

Fig. 8 Compound **10g** and serotonin show interactions with residues at the active site of 5-HT_{1A} receptors.

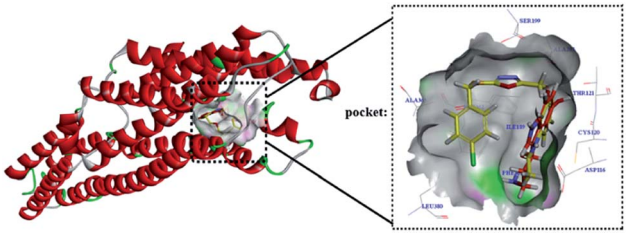

Fig. 9 3D model of 5-HT_{1A} receptor homology model, compound **10g** (yellow) and serotonin (red) in the active binding pocket of 5-HT_{1A} receptor.

The docking results of compound **10g** (Libdock Score: 119.81) showed that it showed hydrogen bond with Asp116, Thr121, and Ser199; π–π stacking with Phe361 and Phe362; and π–alkyl interaction with Cys120, Ile189, Ala 203, and Ala365 (Fig. 8). The docking results of serotonin (Libdock Score: 88.84) showed that it showed hydrogen bond with Thr121, and Asn 386; pi–pi stacking with Phe361; and pi–alkyl interaction with Asp 116, Val 117, Cys120, and Ala 203 (Fig. 8). Results of compound **10g** and serotonin in the active binding pocket of the 5-HT_{1A} receptor are shown in Fig. 9. By analyzing the docking results of compound **10g**, it can be speculated that the compound **10g** can bind well with active site of 5-HT_{1A} receptor, thereby exerting an antidepressant effect.

2.2.8. Prediction of physicochemical and pharmacokinetic properties. Lipinski's "Rule of Five", which is commonly used in drug design and screening, takes into consideration the

Table 3 Drug-likeness parameters of target compounds

Compds	MW[a]	*C* log *P*	*n*HBD	*n*HBA	TPSA
5a	333.11	2.00	1	5	72.28
5b	347.13	2.53	1	5	72.28
5c	361.15	3.06	1	5	72.28
5d	375.16	3.59	1	5	72.28
5e	367.10	1.98	1	5	72.28
5f	385.09	2.13	1	5	72.28
5g	401.06	2.70	1	5	72.28
5h	435.09	2.87	1	5	72.28
5i	381.11	2.48	1	5	72.28
10a	355.10	1.85	1	5	72.28
10b	373.09	1.99	1	5	72.28
10c	373.09	1.99	1	5	72.28
10d	373.09	1.99	1	5	72.28
10e	389.06	2.56	1	5	72.28
10f	389.06	2.56	1	5	72.28
10g	389.06	2.56	1	5	72.28
10h	423.09	2.73	1	5	72.28
10i	423.09	2.73	1	5	72.28
10j	423.09	2.73	1	5	72.28
10k	369.11	2.35	1	5	72.28
10l	369.11	2.35	1	5	72.28
10m	369.11	2.35	1	5	72.28

[a] MW, molecular weight; *C* log *P*, calculated lipophilicity; *n*HBD, number of hydrogen bond donors; *n*HBA, number of hydrogen bond acceptors; TPSA, topological polar surface area; *n*RotB, number of rotatable bonds.

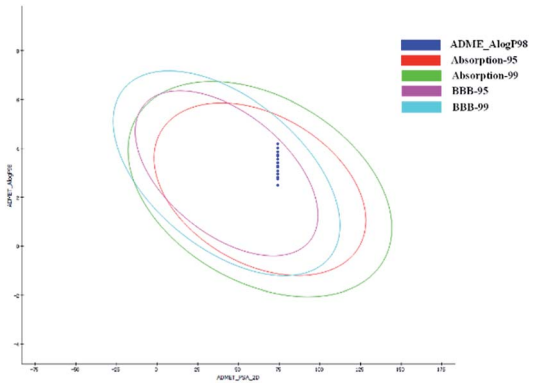

Fig. 10 Target compounds **5a–i** and **10a–m** ADME/T value prediction. The blue dots in the four circular circles indicate that the compound has good pharmacokinetic properties, such as good ABS and favorable BBB permeability.

following aspects: molecular weight (MW ≤ 500), number of hydrogen donors (*n*HBD ≤ 5), number of rotatable bonds (RotB ≤ 10), LogP ≤ 5, and the number of acceptors (*n*HBA ≤ 10). In fact, a compound that meets Lipinski's "Rule of Five" is more likely to be a suitable drug, even in the case of antidepressant drugs. We used DS 2019 to predict the physicochemical properties of the target compounds. As shown in Table 3, almost all target compounds met Lipinski's "Rule of Five". Simultaneously, DS 2019 was used to predict the polar surface area (TPSA) of the target compounds, and the TPSA of all target compounds was shown to be less than 140 (TPSA is an indicator to examine the bioavailability of drugs; TPSA > 140 is considered to indicate low oral bioavailability).[15]

In order to ensure that the compound has good pharmacokinetic properties, the ADME/T module in the DS 2019 software package is used to predict the pharmacokinetic properties of target compounds **5a–i** and **10a–m** (*e.g.* absorption, blood–brain barrier permeability) to avoid the compound's difficulty in penetrating the blood–brain barrier (BBB), low solubility and low oral bioavailability. The prediction results showed that all target compounds exhibited good absorption (ABS) and favorable BBB permeability (Fig. 10).

3. Experimental section

3.1 Chemistry

X-4 binocular microscope melting point apparatus was used to determine the melting point of the compound. The target compound was measured by dissolving in $CDCl_3$ or $DMSO_{d6}$, and tetramethylsilane was selected as an internal standard. ^1H and ^{13}C spectrum data were measured by a Bruker AV-300 nuclear magnetic resonance spectrometer. Abbreviations of spectral data are as follows: s, singlet; d, doublet; t, triplet; q, quartet; m, multiplet). Infrared (IR) is measured by an FT-IR1730 infrared spectrophotometer using the KBr tablet method. High-resolution mass spectra (HRMS) was determined by the mass spectrometer produced by Bruker Daltonik in the Germany. The solvent and reagent used were of analytical or chemical grade (Aladdin, China Reagent Network, Shenyang Chemical Reagent Factory, Sigma-Aldrich). The silica gel used for thin-layer plates and column chromatography was produced by Qingdao Ocean Chemical Factory.

3.1.1. Synthesis of intermediates 2 and 7. 7-Hydroxy-3,4-dihydroquinolin-2(1*H*)-one/*N*-(3-hydroxyphenyl)acetamide (10.0 mmol) and K_2CO_3 (11.0 mmol) were added to a 100 ml single-necked round bottom flask; to this, 30 ml CH_3CN was added and the mixture was stirred at 70 °C for 0.5 h. After 0.5 h, methyl bromoacetate (10.5 mmol) was added to continue the reaction for 6 h. The reaction was followed by thin layer chromatography (TLC) detection. After the reaction was completed, the solvent was pumped off under reduced pressure *in vacuo* to obtain a brown solid. Next, 30 ml of water was added to the round bottom flask, and then the solution was stirred for 10 min, filtered with suction, washed three times with water, and dried to obtain intermediates **2** and **7**.

3.1.2. Synthesis of intermediates 3 and 8. Intermediate **2**/**7** (10.0 mmol) and hydrazine hydrate (11.0 mmol) were added to a 100 ml single-necked round bottom flask, then 30 ml of THF was added, and the reaction was stirred at reflux for 2 h. TLC detection followed the reaction. After the reaction was completed, the excess THF was evaporated under vacuum to obtain the crude product. Add 10 ml CH_3OH to the solid, stirred for 5 min, suction filtered, washed with cooled CH_3OH, dried to obtain intermediates **3** and **8**.

3.1.3. Synthesis of intermediates 4 and 9. Add intermediate **3**/**8** (10.0 mmol), NaOH (15.0 mmol) and CS_2 (20.0 mmol) to a 100 ml single-necked round bottom flask, then add 30 ml EtOH, stir the reaction at 80 °C for 12 h, then add CS_2 (5.0 mmol) continued to react for 7 h. TLC detection tracking reaction, after the completion of the reaction, add 10% HCl solution to adjust the pH to 4–5, until a large amount of white solid precipitated. Suction filtration, washed 3 times with water to obtain a white solid, and dried to obtain intermediates **4** and **9**.

3.1.4. Synthesis of target compounds 5a–i and 10a–m. Intermediate **4**/**9** (10.0 mmol) and K_2CO_3 (11.0 mmol) were added to a 100 ml single-necked round bottom flask, then 30 ml of acetone was added, and the reaction was stirred at 65 °C for 1 h. Then bromine (10.5 mmol) was added to continue the reaction for 9 h. The reaction was tracked by TLC detection. After the reaction was completed, the solvent was vacuum dried under reduced pressure to obtain a white solid. To the white solid was added 30 ml of water, stirred for 10 min, filtered with suction, washed with water 3 times, dried, purified by column chromatography ($CH_3OH : CH_2Cl_2 = 1 : 100$) to obtain the target compounds **5a–i** and **10a–m**.

7-((5-(Butylthio)-1,3,4-oxadiazol-2-yl)methoxy)-3,4-dihydroquinolin-2(1*H*)-one (5a)

Yield: 56%. M_p: 184–185 °C. ^{1}H-NMR ($CDCl_3$, 400 MHz, ppm) δ: 8.42 (s, 1H, CONH), 6.48–7.09 (m, 3H, Ar-H), 5.20 (s, 2H, OCH_2), 3.26 (t, 2H, J = 8.0 Hz, SCH_2), 2.91 (t, 2H, J = 8.0 Hz, $COCH_2$), 2.62 (t, 2H, J = 8.0 Hz, $COCH_2\underline{CH_2}$), 1.43–1.82 (m, 4H, CH_2), 0.95 (t, 3H, J = 8.0 Hz, CH_3). ^{13}C NMR (100 MHz, $CDCl_3$) δ: 171.7, 166.5, 162.9, 157.0, 138.4, 128.9, 117.48, 108.7, 102.8, 59.9, 32.2,

31.1, 30.8, 24.6, 21.7, 13.5. IR (KBr, cm^{-1}): 1673 (C=O). ESI-HRMS calcd for $C_{16}H_{20}N_3O_3S^+$ ($[M + H]^+$): 334.1220; found: 334.1216.

7-((5-(Pentylthio)-1,3,4-oxadiazol-2-yl)methoxy)-3,4-dihydroquinolin-2(1*H*)-one (5b)

Yield: 47%. M_p: 191–192 °C. ^{1}H-NMR ($CDCl_3$, 400 MHz, ppm) δ: 7.94 (s, 1H, CONH), 6.44–7.09 (m, 3H, Ar-H), 5.19 (s, 2H, OCH_2), 3.25 (t, 2H, J = 8.0 Hz, SCH_2), 2.91 (t, 2H, J = 8.0 Hz, $COCH_2$), 2.62 (t, 2H, J = 8.0 Hz, $COCH_2\underline{CH_2}$), 1.32–1.84 (m, 6H, CH_2), 0.91 (t, 3H, J = 8.0 Hz, CH_3). ^{13}C NMR (100 MHz, $DMSO_{d6}$) δ: 170.7, 165.3, 164.0, 156.8, 139.8, 129.0, 117.5, 107.9, 102.8, 59.9, 32.4, 31.0, 30.4, 29.0, 24.4, 22.0, 14.2. IR (KBr, cm^{-1}): 1677 (C=O). ESI-HRMS calcd for $C_{17}H_{22}N_3O_3S^+$ ($[M + H]^+$): 348.1376; found: 348.1372.

7-((5-(Hexylthio)-1,3,4-oxadiazol-2-yl)methoxy)-3,4-dihydroquinolin-2(1*H*)-one (5c)

Yield: 51%. M_p: 176–177 °C. ^{1}H-NMR ($CDCl_3$, 400 MHz, ppm) δ: 7.86 (s, 1H, CONH), 6.43–7.09 (m, 3H, Ar-H), 5.19 (s, 2H, OCH_2), 3.26 (t, 2H, J = 8.0 Hz, SCH_2), 2.91 (t, 2H, J = 8.0 Hz, $COCH_2$), 2.62 (t, 2H, J = 8.0 Hz, $COCH_2\underline{CH_2}$), 1.25–1.83 (m, 8H, CH_2), 0.89 (t, 3H, J = 8.0 Hz, CH_3). ^{13}C NMR (100 MHz, $DMSO_{d6}$) δ: 170.7, 165.3, 164.0, 156.9, 139.8, 129.0, 117.5, 107.9, 102.8, 59.9, 32.4, 31.1, 29.3, 27.9, 24.5, 22.4, 14.3. IR (KBr, cm^{-1}): 1677 (C=O). ESI-HRMS calcd for $C_{18}H_{24}N_3O_3S^+$ ($[M + H]^+$): 362.1533; found: 362.1529.

7-((5-(Heptylthio)-1,3,4-oxadiazol-2-yl)methoxy)-3,4-dihydroquinolin-2(1*H*)-one (5d)

Yield: 44%. M_p: 182–183 °C. ^{1}H-NMR ($CDCl_3$, 400 MHz, ppm) δ: 8.08 (s, 1H, CONH), 6.45–7.09 (m, 3H, Ar-H), 5.19 (s, 2H, OCH_2), 3.25 (t, 2H, J = 8.0 Hz, SCH_2), 2.91 (t, 2H, J = 8.0 Hz, $COCH_2$), 2.62 (t, 2H, J = 8.0 Hz, $COCH_2\underline{CH_2}$), 1.27–1.84 (m, 10H, CH_2), 0.88 (t, 3H, J = 8.0 Hz, CH_3). ^{13}C NMR (100 MHz, $DMSO_{d6}$) δ: 170.7, 165.3, 164.0, 156.8, 139.8, 129.0, 117.5, 107.9, 102.8, 59.9, 32.4, 31.5, 31.0, 29.3, 28.5, 28.2, 24.4, 22.5, 14.4. IR (KBr, cm^{-1}): 1674 (C=O). ESI-HRMS calcd for $C_{19}H_{26}N_3O_3S^+$ ($[M + H]^+$): 376.1689; found: 376.1686.

7-((5-(Benzylthio)-1,3,4-oxadiazol-2-yl)methoxy)-3,4-dihydroquinolin-2(1*H*)-one (5e)

Yield: 48%. M_p: 195–196 °C. ^{1}H-NMR ($CDCl_3$, 400 MHz, ppm) δ: 10.10 (s, 1H, CONH), 6.52–7.43 (m, 8H, Ar-H), 5.31 (s, 2H, OCH_2), 4.51 (s, 2H, SCH_2), 2.79 (t, 2H, J = 8.0 Hz, $COCH_2$), 2.42 (t, 2H, J = 8.0 Hz, $COCH_2\underline{CH_2}$). ^{13}C NMR (100 MHz, $CDCl_3$) δ: 170.7, 164.7, 164.2, 156.8, 139.8, 136.8, 129.4, 129.4, 129.0, 129.0, 128.2, 117.5, 107.9, 102.8, 59.9, 36.2, 31.0, 24.4. IR (KBr, cm^{-1}): 1674 (C=O). ESI-HRMS calcd for $C_{19}H_{18}N_3O_3S^+$ ($[M + H]^+$): 368.1063; found: 368.1061.

7-((5-((4-Fluorobenzyl)thio)-1,3,4-oxadiazol-2-yl)methoxy)-3,4-dihydroquinolin-2(1*H*)-one (5f)

Yield: 42%. M_p: 171–172 °C. ^{1}H-NMR ($CDCl_3$, 400 MHz, ppm) δ: 10.09 (s, 1H, CONH), 7.08–7.48 (dd, 4H, J = 3.0 Hz, J = 3.0 Hz, Ar-H), 6.52–7.16 (m, 3H, Ar–H), 5.31 (s, 2H, OCH_2), 4.51 (s, 2H, SCH_2), 2.79 (t, 2H, J = 8.0 Hz, $COCH_2$), 2.42 (t, 2H, J = 8.0 Hz, $COCH_2\underline{CH_2}$). ^{13}C NMR (100 MHz, $CDCl_3$) δ: 170.7, 164.6, 164.2, 163.2 (d, $^1J_{c-f}$ = 243.0 Hz), 156.8, 139.8, 133.2 (d, $^3J_{c-f}$ = 3.0 Hz), 131.6, 131.6, 131.5, 131.5, 129.0, 117.5, 115.9 (d, $^2J_{c-f}$ = 21.0 Hz), 107.9, 102.7, 59.9, 35.4, 31.0, 24.4. IR (KBr, cm^{-1}): 1674 (C=O). ESI-HRMS calcd for $C_{19}H_{17}FN_3O_3S^+$ ($[M + H]^+$): 386.0969; found: 386.0967.

7-((5-((4-Chlorobenzyl)thio)-1,3,4-oxadiazol-2-yl)methoxy)-3,4-dihydroquinolin-2(1*H*)-one (5g)

Yield: 43%. M_p: 188–189 °C. ^{1}H-NMR ($CDCl_3$, 400 MHz, ppm) δ: 10.09 (s, 1H, CONH), 7.35–7.45 (dd, 4H, J = 4.0 Hz, J = 4.0 Hz, Ar-H), 6.51–6.62 (m, 3H, Ar-H), 5.31 (s, 2H, OCH_2), 4.50 (s, 2H, SCH_2), 2.79 (t, 2H, J = 8.0 Hz, $COCH_2$), 2.42 (t, 2H, J = 8.0 Hz, $COCH_2\underline{CH_2}$). ^{13}C NMR (100 MHz, $CDCl_3$) δ: 170.7, 164.5, 164.3, 156.8, 139.8, 136.1, 132.8, 131.3, 131.3, 129.0, 128.9, 128.9, 117.5, 107.9, 102.7, 59.9, 35.4, 31.0, 24.4. IR (KBr, cm^{-1}): 1672 (C=O). ESI-HRMS calcd for $C_{19}H_{17}ClN_3O_3S^+$ ($[M + H]^+$): 402.0674; found: 402.0670.

7-((5-((4-Trifluoromethylbenzyl)thio)-1,3,4-oxadiazol-2-yl)methoxy)-3,4-dihydroquinolin-2(1*H*)-one (5h)

Yield: 37%. M_p: 199–201 °C. ^{1}H-NMR ($CDCl_3$, 400 MHz, ppm) δ: 7.97 (s, 1H, CONH), 7.54–7.59 (dd, 4H, J = 4.0 Hz, J = 4.0 Hz, Ar-H), 6.43–7.09 (m, 3H, Ar-H), 5.19 (s, 2H, OCH_2), 4.50 (s, 2H, SCH_2), 2.91 (t, 2H, J = 8.0 Hz, $COCH_2$), 2.62 (t, 2H, J = 8.0 Hz, $COCH_2\underline{CH_2}$). ^{13}C NMR (100 MHz, $CDCl_3$) δ: 170.7, 164.4, 156.8, 142.0 (d, $^1J_{c-f}$ = 223.0 Hz), 130.2, 130.2, 130.2, 129.0, 125.8, 125.8, 123.2, 117.5, 107.9, 102.7, 59.9, 35.4, 31.0, 24.4. IR (KBr, cm^{-1}): 1672 (C=O). ESI-HRMS calcd for $C_{20}H_{17}F_3N_3O_3S^+$ ($[M + H]^+$): 436.0937; found: 436.0932.

7-((5-((4-Methylbenzyl)thio)-1,3,4-oxadiazol-2-yl)methoxy)-3,4-dihydroquinolin-2(1*H*)-one (5i)

Yield: 41%. M_p: 182–183 °C. ^{1}H-NMR ($CDCl_3$, 400 MHz, ppm) δ: 8.59 (s, 1H, CONH), 7.12–7.31 (dd, 4H, J = 4.0 Hz, J = 4.0 Hz, Ar-H), 6.49–7.08 (m, 3H, Ar–H), 5.18 (s, 2H, OCH_2), 4.45 (s, 2H, SCH_2), 2.90 (t, 2H, J = 8.0 Hz, $COCH_2$), 2.62 (t, 2H, J = 8.0 Hz, $COCH_2\underline{CH_2}$), 2.33 (s, 3H, CH_3). ^{13}C NMR (100 MHz, $CDCl_3$) δ: 171.8, 165.8, 163.1, 157.0, 138.49, 138.0, 132.1, 129.5, 129.5, 129.0, 129.0, 128.9, 117.4, 108.7, 102.8, 99.9, 59.9, 36.5, 30.8, 24.6, 21.1. IR (KBr, cm^{-1}): 1675 (C=O). ESI-HRMS calcd for $C_{20}H_{20}N_3O_3S^+$ ($[M + H]^+$): 382.1220; found: 382.1217.

N-(3-((5-(Benzylthio)-1,3,4-oxadiazol-2-yl)methoxy)phenyl)acetamide (10a)

Yield: 40%. M_p: 188–189 °C. ^{1}H-NMR ($CDCl_3$, 300 MHz, ppm) δ: 7.52 (s, 1H, CONH), 6.71–7.42 (m, 9H, Ar-H), 5.18 (s, 2H, OCH_2), 4.47 (s, 2H, SCH_2), 2.16 (s, 3H, $COCH_3$). ^{13}C NMR (75 MHz, $CDCl_3$) δ: 168.6, 165.2, 163.4, 157.8, 139.4, 134.4, 131.8, 131.8, 130.7, 130.7, 129.9, 122.1, 113.4, 110.4, 106.5, 59.6, 35.9, 24.5. IR (KBr, cm^{-1}): 1676 (C=O). ESI-HRMS calcd for $C_{18}H_{18}N_3O_3S^+$ ($[M + H]^+$): 356.1063; found: 356.1059.

N-(3-((5-((2-Fluorobenzyl)thio)-1,3,4-oxadiazol-2-yl)methoxy) phenyl)acetamide (10b)

Yield: 62%. M_p: 189–190 °C. ^{1}H-NMR ($CDCl_3$, 300 MHz, ppm) δ: 7.35 (s, 1H, CONH), 6.72–7.50 (m, 8H, Ar-H), 5.19 (s, 2H, OCH_2), 4.49 (s, 2H, SCH_2), 2.16 (s, 3H, $COCH_3$). ^{13}C NMR (75 MHz, $CDCl_3$) δ: 168.5, 163.4, 162.5 (d, $^1J_{c-f}$ = 246.7 Hz), 157.8, 139.3, 131.2 (d, $^3J_{c-f}$ = 3.0 Hz), 130.0 (d, $^2J_{c-f}$ = 8.2 Hz), 129.8, 124.2 (d, $^3J_{c-f}$ = 3.7 Hz), 122.6 (d, $^2J_{c-f}$ = 14.2 Hz), 115.7, 115.4, 113.3, 110.4, 106.4, 59.6, 30.0, 24.5. IR (KBr, cm^{-1}): 1671 (C=O). ESI-HRMS calcd for $C_{18}H_{17}FN_3O_3S^+$ ($[M + H]^+$): 374.0969; found: 374.0966.

N-(3-((5-((3-Fluorobenzyl)thio)-1,3,4-oxadiazol-2-yl)methoxy) phenyl)acetamide (10c)

Yield: 55%. M_p: 174–176 °C. ^{1}H-NMR ($CDCl_3$, 300 MHz, ppm) δ: 7.48 (s, 1H, CONH), 6.71–7.36 (m, 8H, Ar-H), 5.19 (s, 2H, OCH_2), 4.44 (s, 2H, SCH_2), 2.16 (s, 3H, $COCH_3$). ^{13}C NMR (75 MHz, $CDCl_3$) δ: 168.6, 165.2, 164.3 (d, $^1J_{c-f}$ = 245.2 Hz), 157.7, 139.3, 137.7 (d, $^3J_{c-f}$ = 7.5 Hz), 130.3 (d, $^2J_{c-f}$ = 8.2 Hz), 129.8, 124.7 (d, $^3J_{c-f}$ = 3.0 Hz), 116.1 (d, $^2J_{c-f}$ = 22.5 Hz), 115.2, 114.9, 113.4, 110.4, 106.4, 59.6, 36.0, 24.5. IR (KBr, cm^{-1}): 1676 (C=O). ESI-HRMS calcd for $C_{18}H_{17}FN_3O_3S^+$ ($[M + H]^+$): 374.0969; found: 374.0965.

N-(3-((5-((4-Fluorobenzyl)thio)-1,3,4-oxadiazol-2-yl)methoxy) phenyl)acetamide (10d)

Yield: 52%. Mp: 182–183 °C. ^{1}H-NMR ($CDCl_3$, 300 MHz, ppm) δ: 7.52 (s, 1H, CONH), 6.71–7.40 (m, 8H, Ar-H), 5.18 (s, 2H, OCH_2), 4.43 (s, 2H, SCH_2), 2.16 (s, 3H, $COCH_3$). ^{13}C NMR (75 MHz, $CDCl_3$) δ: 168.4, 164.0 (d, $^1J_{c-f}$ = 246.0 Hz), 157.8, 139.3, 131.1 (d, $^3J_{c-f}$ = 3.0 Hz), 130.8 (d, $^2J_{c-f}$ = 8.2 Hz), 129.9, 129.9, 115.8, 115.8, 115.5, 113.3, 110.5, 106.4, 59.6, 35.9, 24.5, 17.2. IR (KBr, cm^{-1}): 1674 (C=O). ESI-HRMS calcd for $C_{18}H_{17}FN_3O_3S^+$ ($[M + H]^+$): 374.0969; found: 374.0965.

N-(3-((5-((2-Chlorobenzyl)thio)-1,3,4-oxadiazol-2-yl)methoxy) phenyl)acetamide (10e)

Yield: 47%. M_p: 176–178 °C. ^{1}H-NMR ($CDCl_3$, 300 MHz, ppm) δ: 7.46 (s, 1H, CONH), 6.71–7.56 (m, 8H, Ar-H), 5.18 (s, 2H, OCH_2), 4.57 (s, 2H, SCH_2), 2.16 (s, 3H, $COCH_3$). ^{13}C NMR (75 MHz, $CDCl_3$) δ: 168.7, 165.5, 163.4, 157.7, 139.4, 134.2, 133.2, 131.3, 129.8, 129.7, 129.6, 127.0, 113.4, 110.3, 106.4, 59.6, 34.4, 24.5. IR (KBr, cm^{-1}): 1673 (C=O). ESI-HRMS calcd for $C_{18}H_{17}ClN_3O_3S^+$ ($[M + H]^+$): 390.0674; found: 390.0670.

N-(3-((5-((3-Chlorobenzyl)thio)-1,3,4-oxadiazol-2-yl)methoxy) phenyl)acetamide (10f)

Yield: 52%. M_p: 191–193 °C. ^{1}H-NMR ($CDCl_3$, 300 MHz, ppm) δ: 7.50 (s, 1H, CONH), 6.71–7.42 (m, 8H, Ar–H), 5.18 (s, 2H, OCH_2), 4.42 (s, 2H, SCH_2), 2.16 (s, 3H, $COCH_3$). ^{13}C NMR (75 MHz, $CDCl_3$) δ: 168.6, 165.1, 163.4, 157.7, 139.3, 137.3, 134.4, 129.9, 129.8, 129.0, 128.3, 127.2, 113.4, 110.4, 106.4, 59.6, 35.9, 24.5. IR (KBr, cm^{-1}): 1675 (C=O). ESI-HRMS calcd for $C_{18}H_{17}ClN_3O_3S^+$ ($[M + H]^+$): 390.0674; found: 390.0670.

N-(3-((5-((4-Chlorobenzyl)thio)-1,3,4-oxadiazol-2-yl)methoxy) phenyl)acetamide (10g)

Yield: 43%. M_p: 195–196 °C. ^{1}H-NMR ($CDCl_3$, 300 MHz, ppm) δ: 7.50 (s, 1H, CONH), 6.71–7.36 (m, 8H, Ar-H), 5.18 (s, 2H, OCH_2), 4.41 (s, 2H, SCH_2), 2.16 (s, 3H, $COCH_3$). ^{13}C NMR (75 MHz, $CDCl_3$) δ: 168.6, 165.2, 163.3, 157.7, 139.4, 133.9, 133.8, 130.4, 130.4, 129.8, 128.8, 128.8, 113.4, 110.3, 106.4, 59.6, 35.8, 24.5. IR (KBr, cm^{-1}): 1671 (C=O). ESI-HRMS calcd for $C_{18}H_{17}ClN_3O_3S^+$ ($[M + H]^+$): 390.0674; found: 390.0669.

N-(3-((5-((2-Trifluoromethylbenzyl)thio)-1,3,4-oxadiazol-2-yl) methoxy)phenyl)acetamide (10h)

Yield: 49%. M_p: 188–189 °C. ^{1}H-NMR ($CDCl_3$, 300 MHz, ppm) δ: 7.65 (s, 1H, CONH), 6.71–7.71 (m, 8H, Ar-H), 5.18 (s, 2H, OCH_2), 4.66 (s, 2H, SCH_2), 2.15 (s, 3H, $COCH_3$). ^{13}C NMR (75 MHz, $CDCl_3$) δ: 168.5, 165.5, 163.5, 157.8, 139.3, 134.0, 132.3, 131.9, 129.8, 128.3, 126.4 (q, J_{c-f} = 5.5 Hz), 125.9, 122.2, 113.4, 110.5, 106.4, 59.6, 33.1, 24.5. IR (KBr, cm^{-1}): 1675 (C=O). ESI-HRMS calcd for $C_{19}H_{17}F_3N_3O_3S^+$ ($[M + H]^+$): 424.0937; found: 424.0933.

N-(3-((5-((3-Trifluoromethylbenzyl)thio)-1,3,4-oxadiazol-2-yl) methoxy)phenyl)acetamide (10i)

Yield: 50%. M_p: 190–192 °C. ^{1}H-NMR ($CDCl_3$, 300 MHz, ppm) δ: 7.69 (s, 1H, CONH), 6.72–7.65 (m, 8H, Ar-H), 5.19 (s, 2H, OCH_2), 4.51 (s, 2H, SCH_2), 2.17 (s, 3H, $COCH_3$). ^{13}C NMR (75 MHz, $CDCl_3$) δ: 168.5, 165.0, 163.4, 157.8, 139.3, 136.4, 132.4, 131.3, 129.8, 129.2, 125.7 (q, J_{c-f} = 11.2 Hz), 125.5, 124.9 (q, J_{c-f} = 11.2 Hz), 113.4, 110.4, 106.4, 59.6, 35.9, 24.5. IR (KBr, cm^{-1}): 1671 (C=O). ESI-HRMS calcd for $C_{19}H_{17}F_3N_3O_3S^+$ ($[M + H]^+$): 424.0937; found: 424.0934.

N-(3-((5-((4-Trifluoromethylbenzyl)thio)-1,3,4-oxadiazol-2-yl) methoxy)phenyl)acetamide (10j)

Yield: 45%. M_p: 176–177 °C. ^{1}H-NMR ($CDCl_3$, 300 MHz, ppm) δ: 7.59 (s, 1H, CONH), 6.72–7.59 (m, 8H, Ar-H), 5.20 (s, 2H, OCH_2), 4.49 (s, 2H, SCH_2), 2.17 (s, 3H, $COCH_3$). ^{13}C NMR (75 MHz, $CDCl_3$) δ: 168.5, 165.0, 163.4, 162.4 (d, $^1J_{c-f}$ = 240.7 Hz), 157.8, 139.5 (d, $^2J_{c-f}$ = 17.2 Hz), 129.9, 129.4, 129.4, 129.4, 125.7, 125.7 (d, $^3J_{c-f}$ = 3.7 Hz), 122.0, 113.3, 110.4, 106.4, 59.6, 35.8, 24.6. IR (KBr, cm^{-1}): 1677 (C=O). ESI-HRMS calcd for $C_{19}H_{17}F_3N_3O_3S^+$ ($[M + H]^+$): 424.0937; found: 424.0933.

N-(3-((5-((2-Methylbenzyl)thio)-1,3,4-oxadiazol-2-yl)methoxy) pheenyl)acetamide (10k)

Yield: 62%. M_p: 176–178 °C. ^{1}H-NMR ($CDCl_3$, 300 MHz, ppm) δ: 7.46 (s, 1H, CONH), 6.73–7.37 (m, 8H, Ar-H), 5.20 (s, 2H, OCH_2), 4.51 (s, 2H, SCH_2), 2.42 (s, 3H, Ar-H), 2.17 (s, 3H, $COCH_3$). ^{13}C NMR (75 MHz, $CDCl_3$) δ: 168.4, 167.7, 163.2, 157.9, 139.3, 137.0, 132.6, 130.7, 130.2, 129.9, 128.5, 126.3, 113.3, 110.5, 106.4, 59.7, 35.0, 24.6, 19.1. IR (KBr, cm^{-1}): 1675 (C=O). ESI-HRMS calcd for $C_{19}H_{20}N_3O_3S^+$ ($[M + H]^+$): 370.1220; found: 370.1215.

***N*-(3-((5-((3-Methylbenzyl)thio)-1,3,4-oxadiazol-2-yl)methoxy) phenyl)acetamide (10l)**

Yield: 65%. M_p: 160–162 °C. ^{1}H-NMR ($CDCl_3$, 300 MHz, ppm) δ: 7.54 (s, 1H, CONH), 6.72–7.35 (m, 8H, Ar-H), 5.18 (s, 2H, OCH_2), 4.44 (s, 2H, SCH_2), 2.33 (s, 3H, Ar-H), 2.16 (s, 3H, $COCH_3$). ^{13}C NMR (75 MHz, $CDCl_3$) δ: 168.4, 165.7, 163.2, 157.9, 139.3, 138.5, 134.9, 129.9, 129.7, 128.9, 128.6, 126.0, 113.3, 110.5, 106.4, 59.7, 36.7, 24.6, 21.2. IR (KBr, cm^{-1}): 1677 (C=O). ESI-HRMS calcd for $C_{19}H_{20}N_3O_3S^+$ ($[M + H]^+$): 370.1220; found: 370.1216.

***N*-(3-((5-((4-Methylbenzyl)thio)-1,3,4-oxadiazol-2-yl)methoxy) phenyl)acetamide (10m)**

Yield: 48%. M_p: 169–170 °C. ^{1}H-NMR ($CDCl_3$, 300 MHz, ppm) δ: 7.34 (s, 1H, CONH), 6.73–7.31 (m, 8H, Ar-H), 5.20 (s, 2H, OCH_2), 4.45 (s, 2H, SCH_2), 2.33 (s, 3H, Ar-H), 2.17 (s, 3H, $COCH_3$). ^{13}C NMR (75 MHz, $CDCl_3$) δ: 168.3, 165.7, 163.1, 157.9, 139.2, 137.9, 132.0, 129.9, 129.4, 129.4, 129.0, 129.0, 113.3, 110.5, 106.3, 59.7, 36.5, 24.6, 21.1, 13.6. IR (KBr, cm^{-1}): 1673 (C=O). ESI-HRMS calcd for $C_{19}H_{20}N_3O_3S^+$ ($[M + H]^+$): 370.1220; found: 370.1215.

3.2 Pharmacology

3.2.1. Animals and treatment. Kunming mice (18–22 g) and Wistar rats (280–300 g) were used for the experiment. All animals were free to move, eat, and drink before the experiment. All animal procedures were performed in accordance with the Guidelines for Care and Use of Laboratory Animals of Liaocheng University and experiments were approved by the Animal Ethics Committee of Liaocheng University (no. 20190312). We dissolved the target compound in 0.5% methylcellulose or dimethyl sulfoxide, and the target compound was administered *via* the intraperitoneal or subcutaneous injection method. Fluoxetine and serotonin were used as the positive control. The antidepressant activity of the target compound was initially screened by FST method (*in vivo)*, and several compounds with potential activity were selected, and the affinity was measured by 5-HT_{1A} binding assay (K_i, *in vitro*). 5-HT ELISA kits test the effect of the most active compound (**10g**) in the two experiments on the concentration of 5-HT in the mice brain. The TST method was used to further verify the *in vivo* antidepressant activity of the best active compound. At the same time, the open-field test method was used to test the effect of the compound on the exploratory activity of experimental mice. DS 2019 or ChemBioDraw Ultra 14.0 was used to predict the physicochemical and pharmacokinetic properties of the target compound.

3.2.2. Antidepressant activity evaluation. Antidepressant activity test were conducted in accordance with previously reported methods: FST model[16] was used for antidepressant activity testing, and the TST model[17,18] was further used for antidepressant activity testing. Through preliminary antidepressant activity test, five compounds (**5g-h**, **10e**, **10g**, and **10j**) with potential activity were selected, and their affinities were determined, which was performed according to previously reported methods (the binding affinity for 5-HT_{1A} receptor was determined by competition binding studies with [^{3}H] 8-OH-DPAT using racemic 8-OH-DPAT as the reference compound), with a slight modification (10 μg membrane protein, 1 nM [^{3}H] 8-OH-DPAT, buffer containing 50 mM Tris-HCl (pH 7.4), 10 mM $MgSO_4$, 0.5 mM EDTA and 0.1% ascorbic acid).[19] Among these compounds, compound **10g**, which showed high activity, was assessed for its effect on the 5-HT concentration in the mice. The 5-HT content was measured according to previously reported method.[7] In order to evaluate the exploratory activity of the animals, the spontaneous activity of compound **10g** was tested in the open-field test.[20]

3.2.3. Molecular docking studies, physicochemical, and pharmacokinetic property prediction. In this study, we selected the FASTA sequence of four 5-HT_{1A} receptors with high homology from RCSB-PDB (web site: https://www.rcsb.org/) (PDB: 4IAQ, 6G79, 4IAR, and 5V54). Then, 2019 DS software was used to construct a homology model of 5-HT_{1A} receptor. The molecular docking module (CDOCKER) in the DS 2019 software was used for docking, and the highest score in the CDOCKER score was analyzed. DS 2019 and ChemBioDraw Ultra 14.0 were used to construct the target compound's structural formula and predict the physicochemical and pharmacokinetic properties, such as MW, RotB, CLogP, nHBD, nHBA, TPSA, ABS level, and BBB permeability level of the target compound.

3.2.4. Statistical analysis. Data are expressed as mean ± standard deviation. One-way analysis of variance (ANOVA) was performed using GraphPad Prism 5.0 statistical software; $0.01 < p < 0.05$ indicated statistically significant differences, $p < 0.01$ indicated highly significant differences.

4. Conclusions

In this study, we designed and synthesized two series of 1,3,4-oxadiazole derivatives as new antidepressant compounds. Most of the compounds showed significant antidepressant effects at dose of 40 mg kg^{-1}. Especially, compound *N*-(3-((5-((4-chlorobenzyl)thio)-1,3,4-oxadiazol-2-yl)methoxy)phenyl) acetamide (**10g**), showed the best antidepressant activity in FST model, similar to the activity of positive drug fluoxetine. The 5-HT_{1A} receptor binding assay showed compound **10g** as the most suitable compound, with an value of $K_i = 1.52$ nM and high binding to 5-HT_{1A} receptors. The results of the *in vivo* 5-HT concentration estimation in mice showed that compound **10g** may have an effect on the mice brain, it can increase the concentration of 5-HT in the brain of mice. In the open-field test, compound **10g** did not affect spontaneous activity. Molecular docking showed that compound **10g** had significant interaction with the amino acid residues around the active site of 5-HT_{1A} receptors. Prediction of the physicochemical and pharmacokinetic properties of the target compounds using DS 2019 and CHEMDRAW 14.0 software showed that all compounds had good physicochemical properties, as well as good BBB permeability and bioavailability.

Conflicts of interest

There are no conflicts to declare.

Acknowledgements

This work was supported by the Natural Science Foundation of Shandong (No. ZR2017BH037); National Natural Science Foundation of China (No. 21675071, 31701827 and 81803360); Youth Innovative Science and Technology Program of Shandong Colleges and University (2019KJM012); The Open Project of Shandong Collaborative Innovation Center for Antibody Drugs (No. CIC-AD1817, CIC-AD1820, CIC-AD1825).

Notes and references

1 J. Olesen, P. Sobscki, T. Truelsen, D. Sestoft and B. Jonsson, *Nord. J. Psychiatry*, 2008, **62**, 114.
2 P. Andlin-Sobocki, B. Jonsson, H. U. Wittchen and J. Olesen, *Eur. Med. J., Neurol.*, 2005, **12**, 1.
3 J. M. Ferguson, *Prim. Care Companion J. Clin. Psychiatry*, 2001, **3**, 22.
4 H. M. Vasiliadis, E. Latimer, P. A. Dionne and M. Préville, *Can. J. Psychiatry*, 2013, **58**, 201.
5 P. Singh, P. K. Sharma, J. K. Sharma, A. Upadhyay and N. Kumar, *Org. Med. Chem. Lett.*, 2012, **2**, 8.
6 X. Q. Deng, M. X. Song, Y. Zheng and Z. S. Quan, *Eur. J. Med. Chem.*, 2014, **73**, 217.
7 S. B. Wang, H. Liu, G. Y. Li, J. Li, X. J. Li, K. Lei, L. C. Wei, Z. S. Quan, X. K. Wang and R. M. Liu, *Pharmacol. Rep.*, 2019, **71**, 1244.
8 N. S. Goud, S. M. Ghouse, M. Arifuddin, M. Alvala, A. Angeli and C. T. Supuran, *Bioorg. Chem.*, 2019, **87**, 765.
9 J. H. Meyer, S. McMain, S. H. Kennedy, L. Korman, G. M. Brown, J. N. DaSilva, A. A. Wilson, T. Blak, R. Eynan-Harvey, V. S. Goulding, S. Houle and P. Links, *Am. J. Psychiatry*, 2003, **160**, 90.
10 P. M. Galdino, M. V. Nascimento, B. L. Sampaio, R. N. Ferreira, J. R. Paula and E. A. Costa, *J. Ethnopharmacol.*, 2009, **124**, 581.
11 H. Sakakibara, K. Ishida, O. Grundmann, J. Nakajima, S. Seo, V. Butterweck, Y. Minami, S. Saito, Y. Kawai, Y. Nakaya and J. Terao, *Biol. Pharm. Bull.*, 2006, **29**, 1767.
12 K. Ostrowska, D. Grzeszczuk, M. Głuch-Lutwin, A. Grybos, A. Siwek, A. Lesniak, M. Sacharczuk and B. Trzaskowsk, *Bioorg. Med. Chem.*, 2018, **26**, 527.
13 P. Blier and N. M. Ward, *Biol. Psychiatry*, 2003, **53**, 93.
14 D. R. Sherin, C. K. Geethu, J. Prabhakaran, J. J. Mann, J. S. Dileep and T. K. Manojkumar, *Comput. Biol. Chem.*, 2019, **78**, 108.
15 N. L. Allinger, *J. Am. Chem. Soc.*, 1977, **99**, 8127.
16 R. D. Porsolt, A. Bertin and M. Jalfre, *Arch. Int. Pharmacodyn. Ther.*, 1977, **229**, 327.
17 L. Stéru, R. Chermat, B. Thierry and P. Simon, *Psychopharmacology*, 1985, **85**, 367.
18 M. Chatterjee, P. Verma and G. Palit, *Indian J. Exp. Biol.*, 2010, **48**, 306.
19 Z. S. Gu, Y. Xiao, Q. W. Zhang and J. Q. Li, *Bioorg. Med. Chem. Lett.*, 2017, **27**, 5420.
20 P. J. Elliott, J. Chan, Y. M. Parker and C. B. Nemeroff, *Brain Res.*, 1986, **381**, 259.